© Marine Technology, Vol. 45, No. 4, October 2008, pp. 194–210

Resistance Characteristics of Fishing Boats Series of ITU

Muhsin Aydin[1] and **Aydin Salci**[2]

This paper presents the results of the resistance and propulsion tests carried out during the development of the Fishing Boat Hull Form Series of ITU, providing the means of designing modern fishing boats capable of operating in the Black Sea, Marmara Sea, Aegean Sea, and the Mediterranean Sea. Initially, nine modern hull forms were generated using the hull forms of the traditional Turkish fishing boats. The model resistance tests of these fishing boats were carried out in the lightship, loaded, and highly loaded conditions. In the present paper, these hull forms are introduced, followed by a systematic presentation of comparative results illustrating the scale effects and the extrapolation diagrams, the influence of the block coefficient, the length to beam ratio, the type of stern, the shape of chine and the fore and aft trim on viscous resistance (form factor k), and wave-making resistance (wave-making resistance coefficient C_W). The findings on the effects of some appendages such as the rudder, the heel of the rudder and the stern tube on the viscous resistance (form factor k), and the total resistance (total resistance coefficient C_{Ts}) are also illustrated. Finally, a general discussion of the results obtained from the resistance tests, wake measurement tests, and flow visualization tests are presented.

Keywords: resistance (general); hydrodynamics (hull form); fishing vessels

1. Introduction

THE FISHING BOAT constitutes the most significant component of the fishing industry which in turn is an important activity in the economies of not only countries at varying stages of development, but also of developed countries. The hull forms of fishing boats show considerable variation in various regions of the world, depending on the fishing methods, meteorological and geographical conditions, accumulated knowledge and experience, and also scientific and technological development. The common influence observed in all of these variations originates from the traditional hull forms indigenous to a given region. These hull forms require improvements parallel to the developments in fishing methods, and the model test techniques provide the basis for such undertakings. Fishing boats have been studied extensively in various parts of the world. An example of such work is on the resistance characteristics of a trawler having the prismatic coefficient value of 0.65 (Ridgely-Nevitt 1956). Taking this hull form as the basis, three trawler hull forms having the prismatic coefficient values of 0.5, 0.6, and 0.7 were generated and model tests were carried out to obtain the effects of various parameters on the resistance characteristics (Ridgely-Nevitt 1963). The following results were obtained: the effect of the ratio of beam to draught on resistance is higher than that of the prismatic coefficient, the transom stern and bulbous bow together improve the resistance characteristics at high speeds, and the prismatic coefficient affects resistance significantly. Elsewhere, the resistance and propulsion data for the trawlers were obtained (Doust 1959) and analyzed statistically. The results were used to develop an optimization technique using the hull form coefficients (Doust 1979). In another study, using the resistance data of 570 models tested in various ship model testing laboratories of Europe, US, and Japan, a regression equation with 13 variables was constituted (Hayes & Engvall 1969), together with a regression equation of 72 terms for a model of length 4.9 m and results of some calculations for various Froude numbers. Van Oortmerssen obtained frictional and residuary resistance values using an algorithm based on 970 measurements of resistance data from 93 fishing boats, tugs, and passenger ships (Van Oortmerssen 1973, Van Oortmerssen 1980), where the frictional resistance values were calculated by the formula of ITTC-57 and the residuary resistance was calculated through a regression equation having six hull form parameters. Prifti and Grigoropoulos obtained and presented the model resistance data of traditional Greek hull forms used widely as fishing boats and passenger ships in Greek waters (Prifti & Grigoropoulos 1995). Other regression and comparison studies also exist (Doust et al. 1967, Antoniou 1969).

The fishing boats of Turkish waters can be classified into three types with respect to their properties: these are the Taka, Cektirme, and Alametro types. All these traditional fishing boat hulls are hydrodynamically inefficient to various degrees. Their underwater hull forms are inefficient in terms of resistance and propulsion. These hulls have longitudinal centers of buoyancy situated forward of amidships, the aft hull form and the propeller housing are not suitable for efficient propulsion, and their rudders are ineffective. They do not have enough stern deck area for working and net storage. In the ship model testing laboratory of ITU Naval Architecture and Ocean Engineering Faculty, the resistance and propulsion tests of three traditional Turkish fishing boat models were carried out, and the results were presented (Nutku 1957). The results also included the comparisons of the performance of the three types. Investigating the resistance and propulsion of the Taka and Alametro types, the maximum possible speeds were determined, and hull form and propeller improvements were proposed (Nutku 1962). The resistance and propulsion characteristics concerning the traditional Cektirme type fishing boats were determined in a separate study (Kucuk 1964), where two models of different scales and a full scale boat was used and the velocity values in the boundary layer of the full scale boat was measured. In another study, the fishing boats 7 to 12 meters long, known as

[1] Naval Architecture and Ocean Engineering Faculty, Istanbul Technical University, Istanbul, Turkey.
[2] Maritime Faculty, Istanbul Technical University, Istanbul, Turkey.
Manuscript received at SNAME headquarters June 2007.

"the infantry" type, common in the coastal regions where the Aegean Sea and the Mediterranean Sea meet, were studied. Their current hull forms have been traditionally developed over 90 years. At present, they are built by craftsmen without plans, drawings, or calculations. The first scientific work carried on these boats is the geosim experiments that took place in Lake Koycegiz, where for the first time the hull forms were obtained. During the geosim experiments, the geosim boats had been tested followed by the resistance tests, the wake measurement tests, the self-propulsion tests, and flow visualization tests. Analyses of the resistance tests were extended to obtain results for assessing the laboratory's model test technique and for the improvement of the hydrodynamic design. The wake measurement tests were made at two different waterlines with the help of a Pitot wake rake. The propeller model self-propulsion tests were made in similar conditions to those of the wake measurement tests. The tufts method was used in the flow visualization tests. Using tufts of different colors, the flow separation zones were identified and observed (Kalipci 1995, 1999). In another study, Kukner and Aydin developed a series of fishing boats (Kukner & Aydin 1997) based on the four boats with prismatic coefficients of 0.582, 0.606, 0.625, and 0.649, which were optimized in terms of resistance and propulsion by D. J. Doust. In this case, starting from 27 boats of identical length and 20 boats of various properties, a total number of 540 hull forms were generated by using a computer program. In the second stage of this study, the boats were modeled numerically and the hydrostatic and seakeeping calculations (heave and pitch amplitudes in head seas) were performed. In the third stage, the influence of the geometrical design parameters on ship motions was investigated. Finally, the regression equations were developed, modeling direct calculation paths from the geometrical design parameters to the seakeeping characteristics such as the heave and pitch motions.

In the present paper, the modern hull forms of the fishing boats that are primarily suitable for operations in the Black Sea, Marmara Sea, Aegean Sea, and the Mediterranean Sea were developed, and fundamentally one may regard this study as the continuation of the previous work performed in the same institution (Kafali et al. 1979, Kafali 1980). These fishing boats exhibit improved stability and seakeeping characteristics compared with the traditional boats. Furthermore, the general accommodation plans provide for a wide and effective afterdeck. Their hull forms are generated considering multipurpose fishing characteristics. Free running speed for these fishing boats is about 10 knots. Fishing speeds for these boats are varied between 4 and 5 knots. The production the models and tests were carried out in the Ata Nutku Ship Model Testing Laboratory of ITU Naval Architecture and Ocean Engineering Faculty, with the support of Scientific & Technological Research Council of Turkey.

Ata Nutku Ship Model Testing Laboratory has a number of experimental facilities for carrying out research and development in marine technology that include the large towing tank, the small towing tank, the cavitation tunnel, the circulating water channel, the stability tank, and computational facilities. The large towing tank is equipped with a numerically controlled carriage, resistance, propulsion and open-water propeller dynamometers, and a wave maker. Speeds of up to 6 m/s can be achieved. The main dimensions of the tank are: length = 160 m, breadth = 6 m, depth = 3.4 m. Ship models up to 4.5 m long are used that enable economic and reliable model tests to be conducted for the majority of current ship forms. Self-propulsion and wake field measurements are performed to derive wake quality and propulsion factors as well as standard resistance tests and open-water propeller tests. The cavitation tunnel was designed and manufactured by Kempf-Remmers of Germany where partially or totally cavitating model propellers, hydrofoil sections, and wings can be tested for cavitation both in free stream and in a simulated ship wake. The cavitation tunnel with the largest section dimensions 63 × 35 cm, is suitable for testing all types of profiles and propellers up to 20 cm in diameter. The circulating water channel is largely used for flow observations and specialist tests in steady forward mo-

Nomenclature

B = beam
C_B = block coefficient
C_F = frictional resistance coefficient
C_M = midship section coefficient
C_P = prismatic coefficient
C_T = total resistance coefficient
C_V = viscous resistance coefficient
C_W = wave-making resistance coefficient
C_{WP} = waterplane area coefficient
D = depth
Fn = Forude number
$GZ(\phi)$ = righting arm
k = form factor
KG = center of gravity above keel
KG_{max} = maximum value of KG
$L(L_{WL}, L_{PP})$ = length (length of waterline, length between perpendiculars)
LCB = longitudinal center of buoyancy
R = chine radius
Rn = Reynolds number
RPM = revolution per minute
R_T = total resistance
S_W = wetted surface
t = thrust-deduction coefficient
T = draught
v = ship or model speed (in m/s)
$w(w_T)$ = wake coefficient (Taylor wake fraction)
$X_m = 1/(\log Rn_m - 2)^2$
α = ratio of geometric similarity
Δ = displacement
ϕ = heel angle
η_h = hull efficiency
η_r = relative rotative efficiency
η_o = open-water efficiency
η = propulsion efficiency
∇ = displacement volume

List of abbreviations

3D = three dimensional
BL = base line
CL = center line
D = diagonal
geosim = geometrically similar/geometric similarity
ITTC-57 = International Towing Tank Conference (1957)
ITU = Istanbul Technical University
m = subscript for model
PC-SHCP = Personal Computer-Ship Hull Characteristics Program
RGS = ratio of geometric similarity
s = subscript for ship
WL = waterline

Table 1 Some characteristics of the generated fishing boat forms

Boat No.	Loading Condition	L (m)	B (m)	T (m)	C_B	C_M	C_{WP}	C_P	L/B	B/T	LCB (m) (+ Aft)	S_W (m^2) (without app.)	Δ (kN)
148/1	Lightship	18.50	5.240	1.715	0.342	0.608	0.651	0.563	3.531	3.056	0.43	92.40	571.56
	Loaded	20.00	5.714	2.286	0.378	0.661	0.730	0.572	3.500	2.500	0.83	126.10	992.96
	Highly Loaded	20.34	5.840	2.858	0.441	0.712	0.753	0.619	3.483	2.044	1.18	150.20	1,505.16
148/2	Lightship	18.50	5.714	1.715	0.510	0.857	0.693	0.595	3.238	3.333	–0.32	106.90	929.42
	Loaded	20.00	5.714	2.286	0.535	0.892	0.789	0.600	3.500	2.500	0.01	139.80	1,405.38
	Highly Loaded	20.34	5.714	2.858	0.581	0.914	0.836	0.636	3.560	2.000	0.25	164.00	1,940.20
148/3	Lightship	18.50	5.440	1.715	0.355	0.600	0.659	0.592	3.401	3.173	0.38	92.60	615.93
	Loaded	20.00	5.714	2.286	0.406	0.668	0.727	0.608	3.500	2.500	0.80	125.00	1,066.51
	Highly Loaded	20.34	5.840	2.858	0.457	0.728	0.747	0.628	3.483	2.044	1.09	150.00	1,559.76
148/4	Lightship	18.50	5.714	1.715	0.460	0.851	0.655	0.541	3.238	3.333	–0.34	99.30	838.30
	Loaded	20.00	5.714	2.286	0.497	0.888	0.789	0.560	3.500	2.500	0.02	134.10	1,305.56
	Highly Loaded	20.34	5.714	2.858	0.564	0.911	0.836	0.619	3.560	2.000	0.28	159.06	1,883.43
148/5	Lightship	18.50	5.520	1.715	0.411	0.657	0.688	0.626	3.351	3.220	0.37	99.00	723.57
	Loaded	20.00	5.714	2.286	0.444	0.720	0.745	0.617	3.500	2.500	0.63	131.00	1,166.33
	Highly Loaded	20.34	5.840	2.858	0.494	0.768	0.753	0.643	3.483	2.044	0.91	156.80	1,686.05
148/6	Lightship	21.28	5.440	1.715	0.352	0.600	0.655	0.587	3.912	3.173	0.43	107.90	702.50
	Loaded	22.86	5.714	2.286	0.400	0.668	0.727	0.599	4.001	2.500	0.91	145.50	1,201.01
	Highly Loaded	23.19	5.840	2.858	0.455	0.728	0.749	0.625	3.971	2.044	1.25	173.60	1,770.53
148/7	Lightship	21.28	5.714	1.715	0.454	0.851	0.651	0.533	3.724	3.333	–0.39	112.50	951.70
	Loaded	22.86	5.714	2.286	0.491	0.888	0.789	0.553	4.001	2.500	0.02	152.50	1,474.24
	Highly Loaded	23.19	5.714	2.858	0.549	0.911	0.838	0.603	4.058	2.000	0.32	181.50	2,090.22
148/8	Lightship	27.06	5.440	1.715	0.351	0.600	0.644	0.585	4.974	3.173	0.54	132.60	890.77
	Loaded	28.57	5.714	2.286	0.404	0.668	0.727	0.605	5.000	2.500	1.14	179.40	1,516.01
	Highly Loaded	28.89	5.840	2.858	0.458	0.728	0.751	0.629	4.947	2.044	1.56	214.10	2,220.27
148/9	Lightship	27.06	5.714	1.715	0.449	0.851	0.640	0.528	4.736	3.333	–0.48	132.00	1,196.86
	Loaded	28.57	5.714	2.286	0.493	0.888	0.789	0.555	5.000	2.500	0.03	190.80	1,849.98
	Highly Loaded	28.89	5.714	2.858	0.559	0.911	0.840	0.614	5.056	2.000	0.40	226.60	2,651.42

tion under the atmospheric pressure. The test section of the channel is 1.5 × 0.75 m and the maximum speed is 2 m/s. The channel is equipped with a mechanical resistance dynamometer and Pitot tubes for velocity measurements. Flow visualization tests are also performed frequently using wool tufts or dye injection.

The aforementioned study lasted for approximately 3 years. A fishing boat hull form with transom stern was developed from a form with cruiser stern and denoted as the "parent" fishing boat hull form. Then, based on the parent fishing boat, four hull forms with varying block coefficients C_B from 0.378 to 0.535, were generated in order to investigate the influence of C_B on resistance (especially k and C_W). The generated hull forms were numbered as 148/1 (the parent fishing boat), 148/2, 148/3, 148/4, and 148/5. The lengths of the hull forms 148/3 and 148/4 were extended by increasing the distance between the stations to investigate the effects of L/B on resistance. Thus, the boat forms 148/6 and 148/8 were generated based on the hull form 148/3, with L/B ratios of four and five, respectively. Similarly, boats 148/7 and 148/9 were generated based on the hull form 148/4, with L/B ratios of also four and five, respectively. The lengths of the boats 148/3, 148/6, and 148/8 are 20, 22.86, and 28.57 m, respectively, and the average value of C_B is 0.403. The lengths of the boats 148/4, 148/7, and 148/9 are also 20, 22.86, and 28.57 m, and the average value of C_B is 0.494. Important characteristics of all generated boat forms are given in Table 1. The hull forms (sections) and 3D views of selected generated boat forms are shown in Figs. 1 to 5. In the second stage of the hull form development, 13 hull forms with varying block coefficients were generated using the initial five hull forms whose characteristics are given above. Keeping the body section forms and beams of the boats with the same block coefficient unchanged, additional 26 hull forms with two different L/B ratios were generated by increasing the space between the stations. Thus, a Fishing Boat Hull Form Series that consists of 39 fishing boats in total was obtained (Aydin 2002, Aydin & Salci 2007). The stability analyses of all the fishing boats were completed in the lightship and loaded conditions. The computer program PC-SHCP was used for this purpose. As the centers of gravity of these fishing boats cannot be known exactly, a range of KG that was known to be appropriate was determined. This range of KG

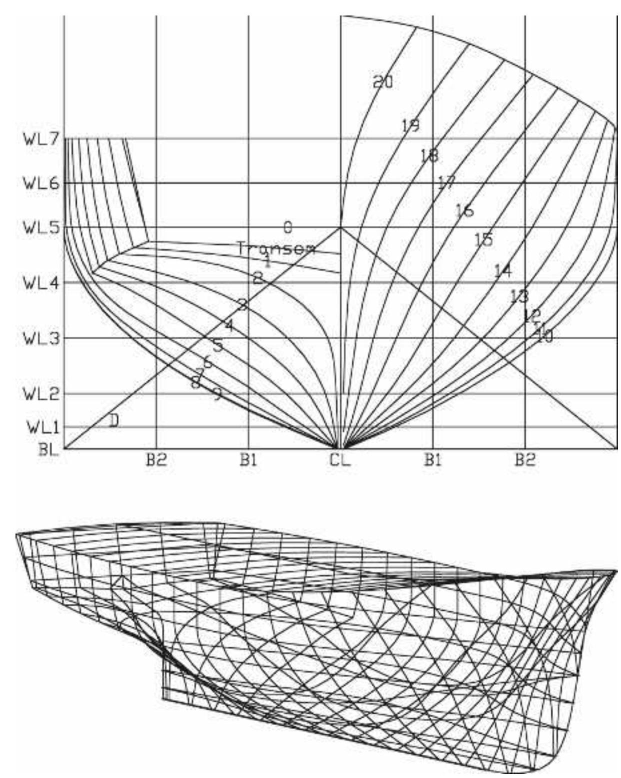

Fig. 1 The body sections and 3D view of the fishing boat 148/1 (L = 20 m and C_B = 0.378)

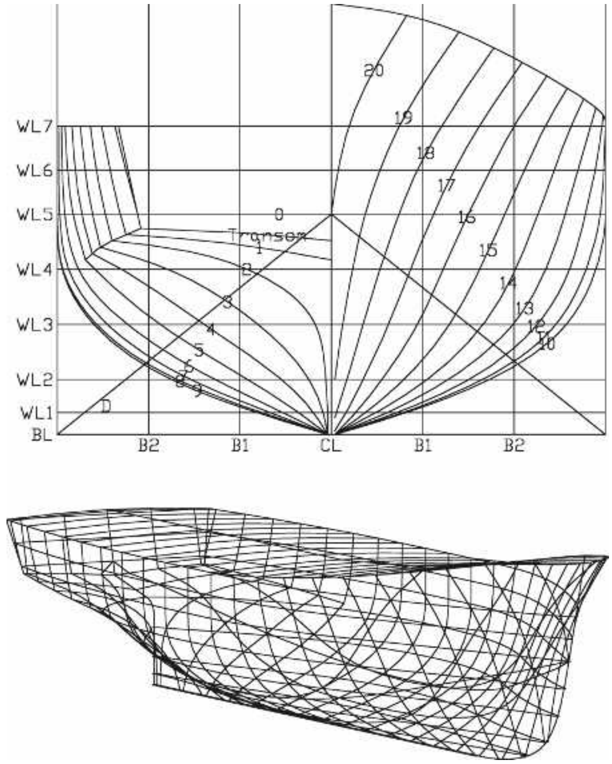

Fig. 2 The body sections and 3D view of the fishing boat 148/5 (L = 20 m and C_B = 0.444)

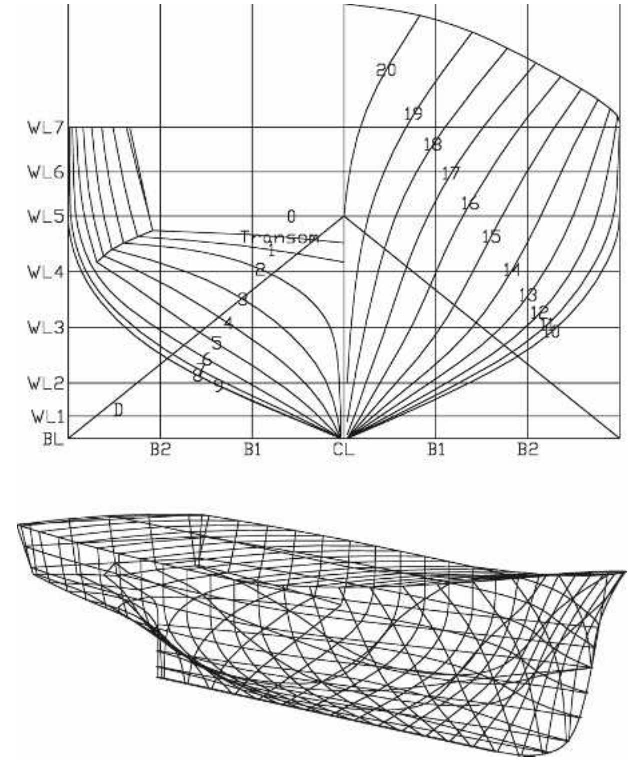

Fig. 4 The body sections and 3D view of the fishing boat 148/6 (L = 22.86 m and C_B = 0.400)

contained a total of 10 values from 2.15 to 2.6 m, with an increment of 0.05 m, which is assumed to be applicable to both the lightship and loaded conditions. Thus, taking into account all the individual members of the Fishing Boat Hull Form Series, the stability parameters for 260 different situations were determined with respect to two different loading conditions and 10 different values of KG. Later, by further investigation into the quantities obtained from the curves of GZ (ϕ) such as the stability criteria and the other stability

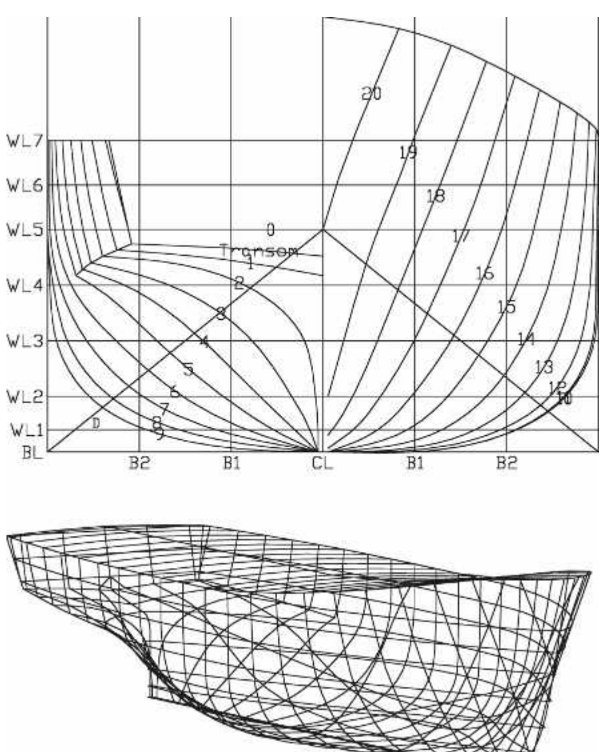

Fig. 3 The body sections and 3D view of the fishing boat 148/2 (L = 20 m and C_B = 0.535)

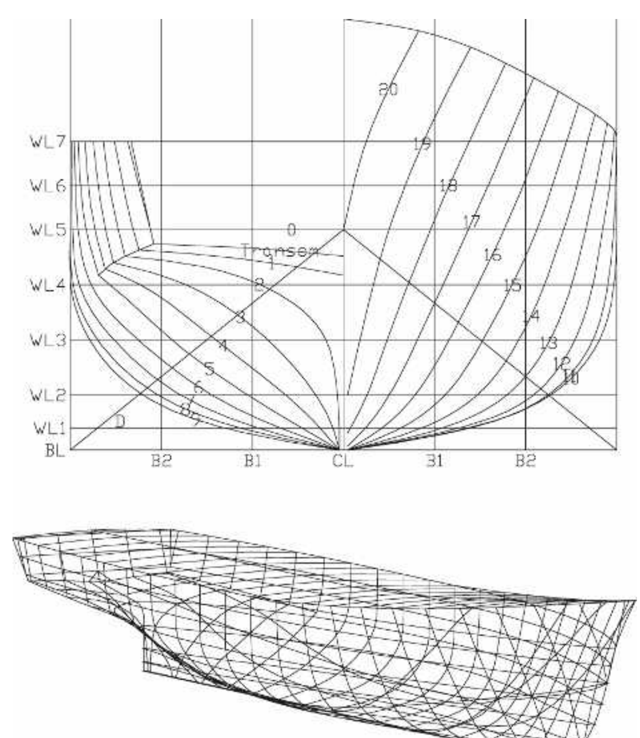

Fig. 5 The body sections and 3D view of the fishing boat 148/9 (L = 28.57 m and C_B = 0.493)

Table 2 Some characteristics of the models used in the tests

Model No.	Loading Condition	L (m)	B (m)	T (m)	C_B	C_M	C_{WP}	C_P	L/B	B/T	LCB (m) (+ Aft)	S_W (m^2) (without app.)	Δ (kN)	Construction Material
148/1B	Lightship	1.850	0.524	0.171	0.342	0.608	0.651	0.563	3.531	3.056	0.043	0.924	0.557	Wood
	Loaded	2.000	0.571	0.229	0.378	0.661	0.730	0.572	3.500	2.500	0.083	1.261	0.968	
	Highly loaded	2.034	0.584	0.286	0.441	0.712	0.753	0.619	3.483	2.044	0.118	1.502	1.467	
148/2B	Lightship	1.850	0.571	0.171	0.510	0.857	0.693	0.595	3.238	3.333	−0.032	1.069	0.906	Paraffin
	Loaded	2.000	0.571	0.229	0.535	0.892	0.789	0.600	3.500	2.500	0.001	1.398	1.370	
	Highly loaded	2.034	0.571	0.286	0.581	0.914	0.836	0.636	3.560	2.000	0.025	1.640	1.891	
148/3B	Lightship	1.850	0.544	0.171	0.355	0.600	0.659	0.592	3.401	3.173	0.038	0.926	0.600	Paraffin
	Loaded	2.000	0.571	0.229	0.406	0.668	0.727	0.608	3.500	2.500	0.080	1.250	1.039	
	Highly loaded	2.034	0.584	0.286	0.457	0.728	0.747	0.628	3.483	2.044	0.109	1.500	1.520	
148/4B	Lightship	1.850	0.571	0.171	0.460	0.851	0.655	0.541	3.238	3.333	−0.034	0.993	0.817	Paraffin
	Loaded	2.000	0.571	0.229	0.497	0.888	0.789	0.560	3.500	2.500	0.002	1.341	1.272	
	Highly loaded	2.034	0.571	0.286	0.564	0.911	0.836	0.619	3.560	2.000	0.028	1.591	1.836	
148/5B	Lightship	1.850	0.552	0.171	0.411	0.657	0.688	0.626	3.351	3.220	0.037	0.990	0.705	Paraffin
	Loaded	2.000	0.571	0.229	0.444	0.720	0.745	0.617	3.500	2.500	0.063	1.310	1.137	
	Highly loaded	2.034	0.584	0.286	0.494	0.768	0.753	0.643	3.483	2.044	0.091	1.568	1.643	
148/6B	Lightship	2.128	0.544	0.171	0.352	0.600	0.655	0.587	3.912	3.173	0.043	1.079	0.685	Paraffin
	Loaded	2.286	0.571	0.229	0.400	0.668	0.727	0.599	4.001	2.500	0.091	1.455	1.171	
	Highly loaded	2.319	0.584	0.286	0.455	0.728	0.749	0.625	3.971	2.044	0.125	1.736	1.726	
148/7B	Lightship	2.128	0.571	0.171	0.454	0.851	0.651	0.533	3.724	3.333	−0.039	1.125	0.928	Paraffin
	Loaded	2.286	0.571	0.229	0.491	0.888	0.789	0.553	4.001	2.500	0.002	1.525	1.437	
	Highly loaded	2.319	0.571	0.286	0.549	0.911	0.838	0.603	4.058	2.000	0.032	1.815	2.037	
148/8B	Lightship	2.706	0.544	0.171	0.351	0.600	0.644	0.585	4.974	3.173	0.054	1.326	0.868	Paraffin
	Loaded	2.857	0.571	0.229	0.404	0.668	0.727	0.605	5.000	2.500	0.114	1.794	1.478	
	Highly loaded	2.889	0.584	0.286	0.458	0.728	0.751	0.629	4.947	2.044	0.156	2.141	2.164	
148/9B	Lightship	2.706	0.571	0.171	0.449	0.851	0.640	0.528	4.736	3.333	−0.048	1.320	1.167	Paraffin
	Loaded	2.857	0.571	0.229	0.493	0.888	0.789	0.555	5.000	2.500	0.003	1.908	1.803	
	Highly loaded	2.889	0.571	0.286	0.559	0.911	0.840	0.614	5.056	2.000	0.040	2.266	2.584	

characteristics, graphical presentations that vary with C_B for two loading conditions and 10 different values of KG were obtained. The variation with respect to C_B of any quantity that characterizes the curve of GZ (ϕ) was represented by a fifth-degree polynomial for any loading condition and any value of KG. Later, the variation with respect to KG of any quantity that characterizes the curve of GZ (ϕ) was represented by a third-degree polynomial. In addition, for two loading conditions and 10 different values of KG, full stability assessments were carried out for all the hull forms. The ratios of the maximum height of the center of gravity above the keel to depth, KG_{max}/D, as a function of C_B were determined in the lightship and loaded conditions as follows (Aydin & Akyildiz 2005):

$$\frac{KG_{max}}{D} = 9.112\, C_B^3 - 14.238\, C_B^2 + 6.812\, C_B - 0.252 \quad \text{(For the lightship condition)} \qquad (1)$$

$$\frac{KG_{max}}{D} = 5.015\, C_B^3 - 6.453\, C_B^2 + 2.077\, C_B + 0.672 \quad \text{(For the loaded condition)} \qquad (2)$$

2. Models used in tests and resistance test analyses

The hull forms generated for the fishing boats given in Table 1 were built in model scale 1/10. The model tests were designed to investigate the influence of the block coefficient and L/B ratio on the form factor and the wave-making resistance coefficient. Various characteristics and the construction material of all the models are given in Table 2.

Besides the model 148/1B, the geosim models 148/1A, 148/1C, and 148/1D of the parent fishing boat 148/1 were built to assess the scale effects and to obtain the extrapolation diagrams. The scale values of these models are 2/25, 3/25, and

Table 3 Some characteristics of the geosim models

Model No.	Scale (1/α)	Loading Condition	L (m)	B (m)	T (m)	C_B	LCB (m) (+ Aft)	S_W (m^2) (without app.)	S_W (m^2) (with app.)	Δ (kN)	Construction Material
148/1A	(2/25)	Lightship	1.480	0.419	0.137	0.342	0.034	0.591	0.613	0.285	Wood
		Loaded	1.600	0.457	0.183	0.378	0.066	0.807	0.831	0.495	
		Highly Loaded	1.627	0.467	0.229	0.441	0.094	0.961	0.985	0.751	
148/1B	(2.5/25)	Lightship	1.850	0.524	0.171	0.342	0.043	0.924	0.958	0.557	Wood
		Loaded	2.000	0.571	0.229	0.378	0.083	1.261	1.299	0.968	
		Highly Loaded	2.034	0.584	0.286	0.441	0.118	1.502	1.540	1.467	
148/1C	(3/25)	Lightship	2.220	0.629	0.206	0.342	0.052	1.331	1.380	0.963	Wood
		Loaded	2.400	0.686	0.274	0.378	0.100	1.816	1.871	1.672	
		Highly Loaded	2.441	0.701	0.343	0.441	0.142	2.163	2.218	2.535	
148/1D	(4/25)	Lightship	2.960	0.838	0.274	0.342	0.069	2.365	2.452	2.282	Wood
		Loaded	3.200	0.914	0.366	0.378	0.133	3.228	3.325	3.964	
		Highly Loaded	3.254	0.934	0.457	0.441	0.189	3.845	3.942	6.009	

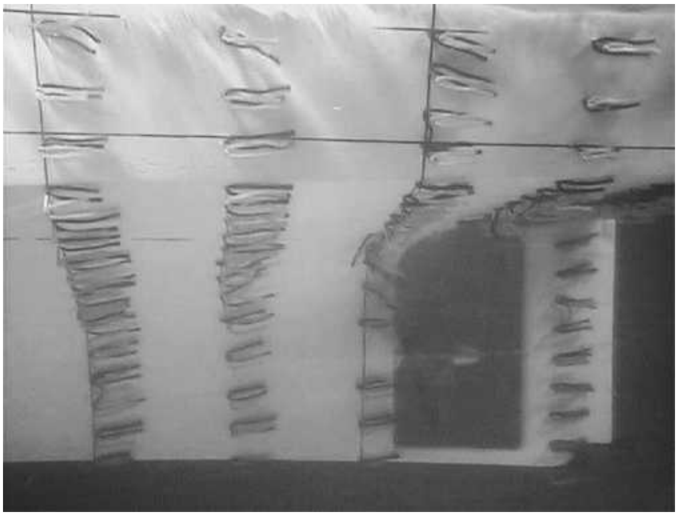

Fig. 6 The appendages on the model 148/1C

4/25, respectively, and their relevant characteristics are given in Table 3.

The models 148/3B(C) and 148/4B(C) of the fishing boats 148/3 and 148/4 were built with the cruiser stern to investigate the effects of the stern geometry on the resistance characteristics. Additionally, the effects of the chine shape on the form factor and the wave-making resistance coefficient were examined by rounding the chine of the model 148/1B. The tests of the models 148/3B and 148/4B were executed in trimmed conditions both by stern and by bow, to investigate the effect of trim on the form factor and the wave-making resistance coefficient. To reveal the influence of the appendages on the form factor and the total resistance coefficient, the tests of the models 148/1A, 148/1B, and 148/1C were repeated with the appendages such as the rudder, the heel of the rudder and the stern tube present (see Fig. 6). All the tests were carried out in the lightship (0.75 × T), loaded (1.00 × T), and highly loaded (1.25 × T) conditions, allowing the effects of beam to draught ratio to be investigated. The raw data (v_m, R_{Tm}) were represented by a spline curve that is tangent to the axis of speed at the origin. Later, an analysis of the smooth test data obtained from the spline curve was performed by using Hughes' method (Aydin 2002).

The equations used in this procedure are given as follows (Salci 1985):

$$C_{Tm} = C_{Vm} + C_{Wm} \tag{3}$$

$$C_{Vm} = (1 + k_m)C_{Fm} \tag{4}$$

$$C_{Fm} = \left(\frac{0.075}{(\log(Rn_m) - 2)^2}\right) \quad (ITTC-57) \tag{5}$$

$$Fn_s = Fn_m = Fn \tag{6}$$

$$C_{Fs} = \left(\frac{0.075}{(\log(Rn_s) - 2)^2}\right) \quad (ITTC-57) \tag{7}$$

$$k_s = k_m = k \tag{8}$$

$$C_{Vs} = (1 + k)\, C_{Fs} \tag{9}$$

$$C_{Ws} = C_{Wm} = C_W \tag{10}$$

$$C_{Ts} = C_{Vs} + C_W \tag{11}$$

The form factor for the model, k_m (in equations 4 and 8) was determined with both modified Hughes' method and Prohaska's method for comparison. In the calculations, however, the form factors appointed by modified Hughes' method were taken into consideration. The resistance characteristics for all the fishing boats were obtained for the ideal conditions. In other words, they are the values that are calculated by assuming perfectly smooth and clean underwater hull form, in the absence of waves and currents in the sea, without any wind and without any air resistance.

The wake measurement tests of the geosim models 148/1B and 148/1C of the parent fishing boat were carried out by Kempf circles method. As a result of these tests, it was found that the nominal wake coefficient varied between 0.22 and

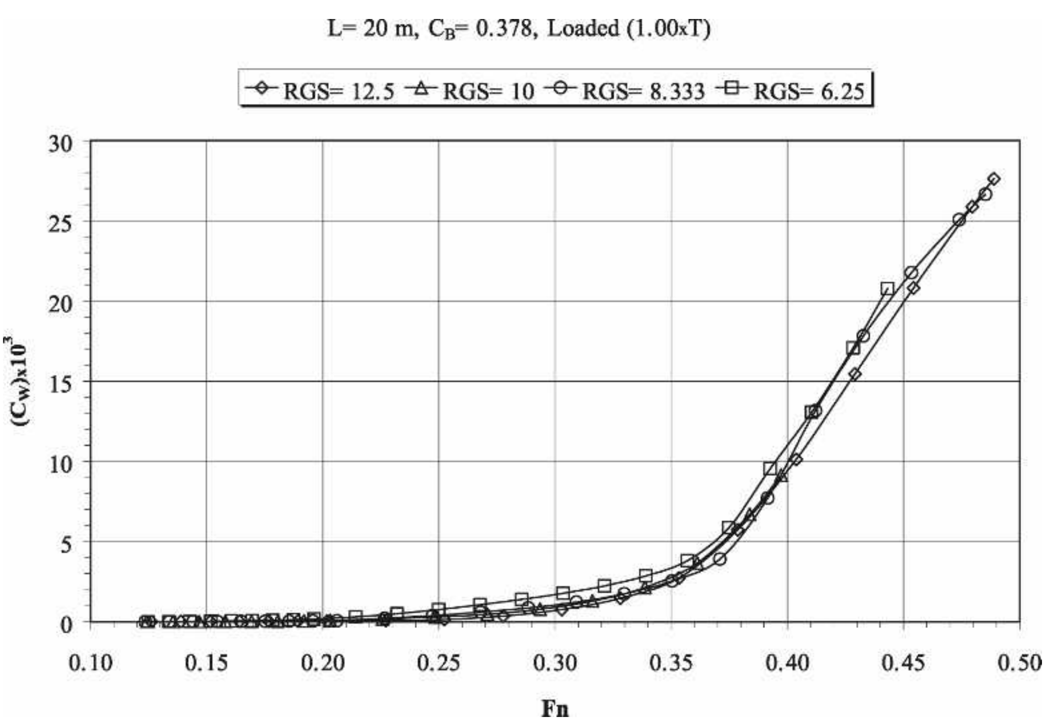

Fig. 7 The variation of wave-making resistance coefficient with Froude number, in the loaded condition

Table 4 The form factors of four models and the average form factors in all loading conditions

	k		
	Lightship (0.75 × T)	Loaded (1.00 × T)	Highly Loaded (1.25 × T)
Model No.			
148/1A	0.263	0.270	0.456
148/1B	0.264	0.258	0.450
148/1C	0.238	0.378	0.594
148/1D	0.345	0.248	0.600
Average Value	**0.278**	**0.289**	**0.525**

0.24, and if the length of the model was increased, the nominal wake coefficient decreased. In addition, the wake measurement tests of the model 148/1C were done in the loaded condition for three different speeds, and the computer-aided analyses of these tests were carried out. Based on the results of these analyses, the wake characteristics for three ship speeds and the variation of the nominal wake coefficient with respect to the ship speed were obtained.

The computer-aided analyses of open-water tests and the self-propulsion tests with the models of the Wageningen B Series 3.50 propeller and a highly skewed propeller were performed. In the self-propulsion tests, the model 148/1D of the parent fishing boat was used. Evaluating the self-propulsion tests with the equivalence thrust method, the self-propulsion characteristics were obtained. These self-propulsion characteristics are: $w = 0.195$, $t = 0.156$, $\eta_h = 1.048$, $\eta_r = 1.002$, $\eta_o = 0.502$, $\eta = 0.528$ for the Wageningen B Series 3.50 propeller and $V_s = 10$ knots and also $w = 0.148$, $t = 0.156$, $\eta_h = 0.990$, $\eta_r = 1.000$, $\eta_o = 0.500$, $\eta = 0.496$ for the highly skewed propeller and $V_s = 10$ knots.

The flow visualization tests of the model 148/1C of the parent fishing boat were carried out in the loaded and highly loaded conditions by using the tuft method.

3. Scale effects and extrapolation diagrams

The scale effects were examined and the extrapolation diagrams were drawn by utilizing the resistance tests analyses of four geosim models of the parent fishing boat in the lightship, loaded and highly loaded conditions. The RGS values of the models 148/1A, 148/1B, 148/1C, and 148/1D are 12.5, 10, 8.333, and 6.25, respectively. The variation of the wave-making resistance coefficient of the parent boat was obtained using Hughes' method to analyze the resistance tests of these models without the appendages. These curves are shown in Fig. 7 for the loaded condition only. The average form factors of these models in three loading conditions are calculated and presented in Table 4. Thus, using two different methods, the extrapolation diagrams are obtained for three loading conditions. Selected diagrams referring to the loaded condition only are shown in Figs. 8 and 9.

4. Effects of block coefficient

The results of the resistance tests of the models 148/1B, 148/2B, 148/3B, 148/4B, and 148/5B in the lightship, loaded, and highly loaded conditions were used to investigate the effects of the block coefficient on the form factor and the wave-making resistance coefficient. The distribution with respect to the block coefficient, of the form factors of all the models in the loaded condition is given in Fig. 10. The variation with the Froude number of the wave-making resistance coefficient of the generated hull forms and the parent form with different block coefficients are shown in Fig. 11 for the loaded condition only.

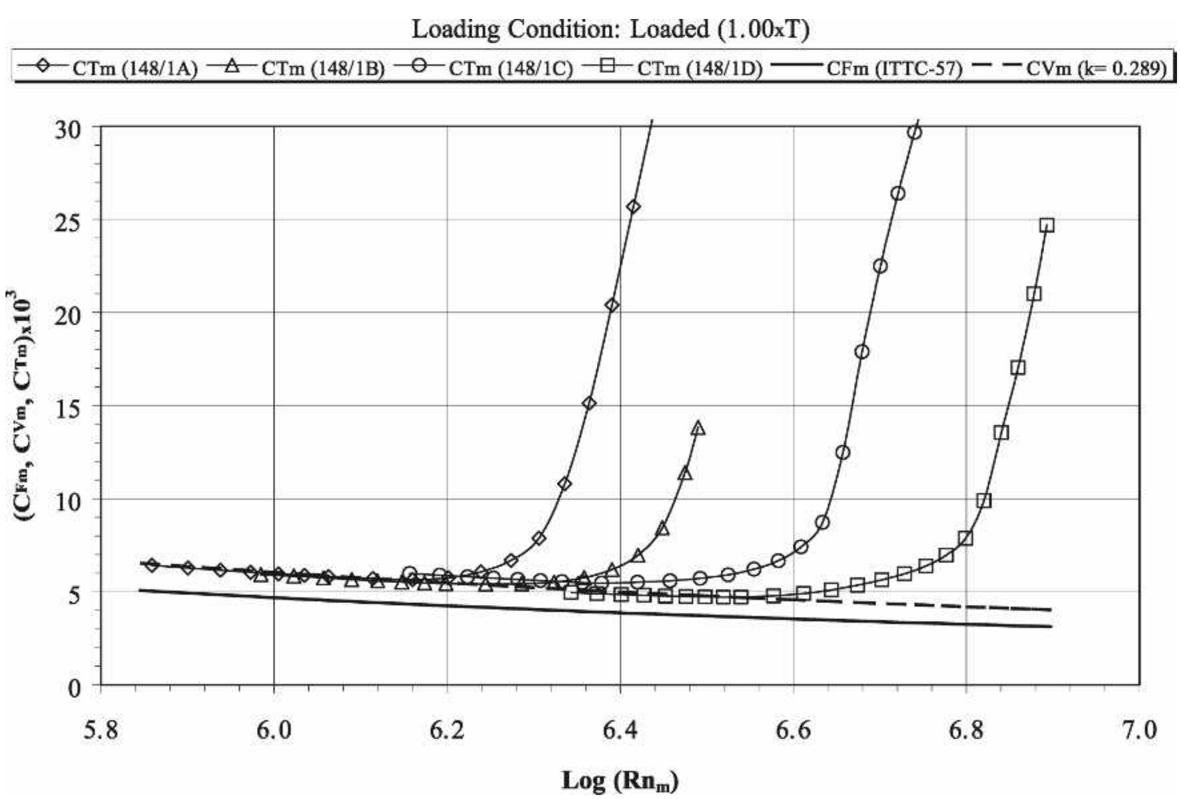

Fig. 8 The extrapolation diagram in the loaded condition

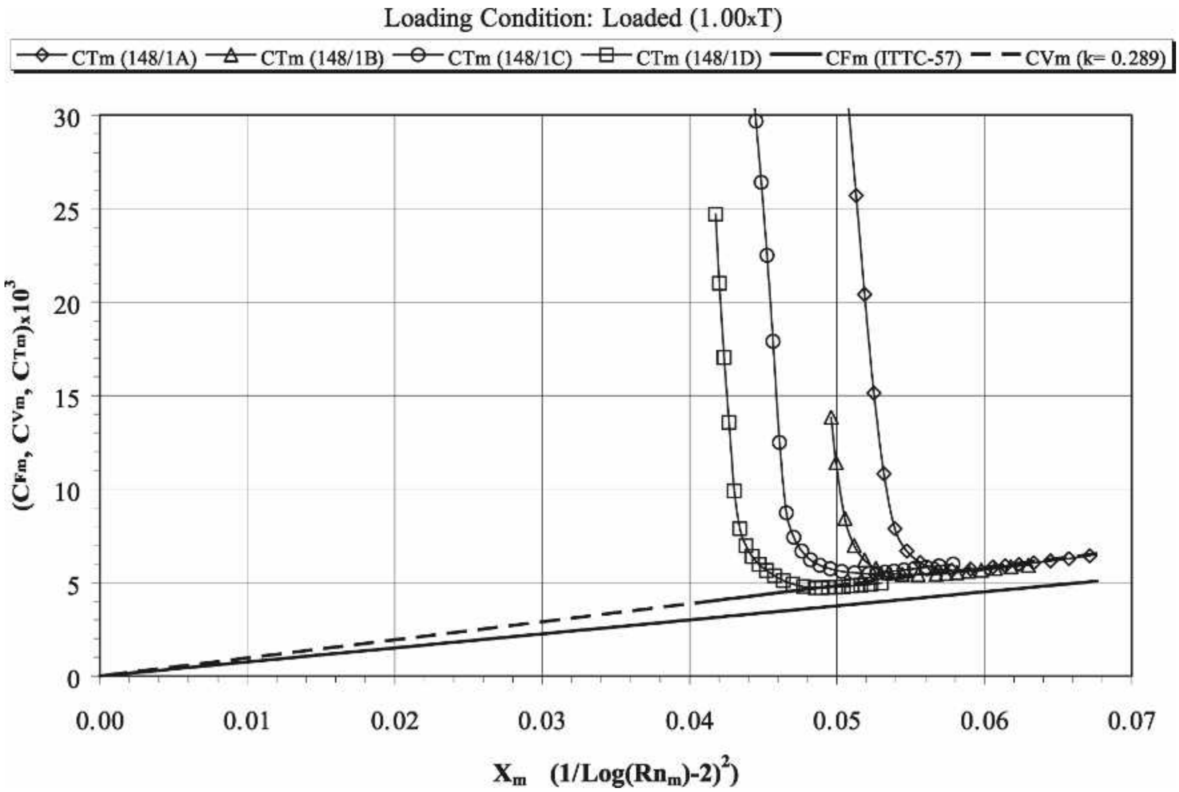

Fig. 9 The extrapolation diagram obtained by the modified Hughes' method in the loaded condition

5. Effects hull length to beam ratio

The influence of the ratio of L/B on the form factor and the wave-making resistance coefficient was investigated by analyzing the resistance tests data of the models 148/3B, 148/6B, 148/8B and 148/4B, 148/7B, 148/9B. The average value of C_B for the models 148/3B, 148/6B, and 148/8B is 0.403. Meanwhile, the average value of C_B for the models 148/4B, 148/7B, and 148/9B is 0.494. Keeping the form of the body sections of the models 148/3B and 148/4B unchanged, but increasing the spacing between the stations, the models 148/6B, 148/8B, and 148/7B, 148/9B were constructed. The ratio L/B for the models 148/6B and 148/7B is four, whereas for the models 148/8B and 148/9B it is five. These L/B ratios correspond to ship lengths of 20, 22.86, and 28.57 m in the full scale for both values of C_B, 0.403 and 0.494. For the light-

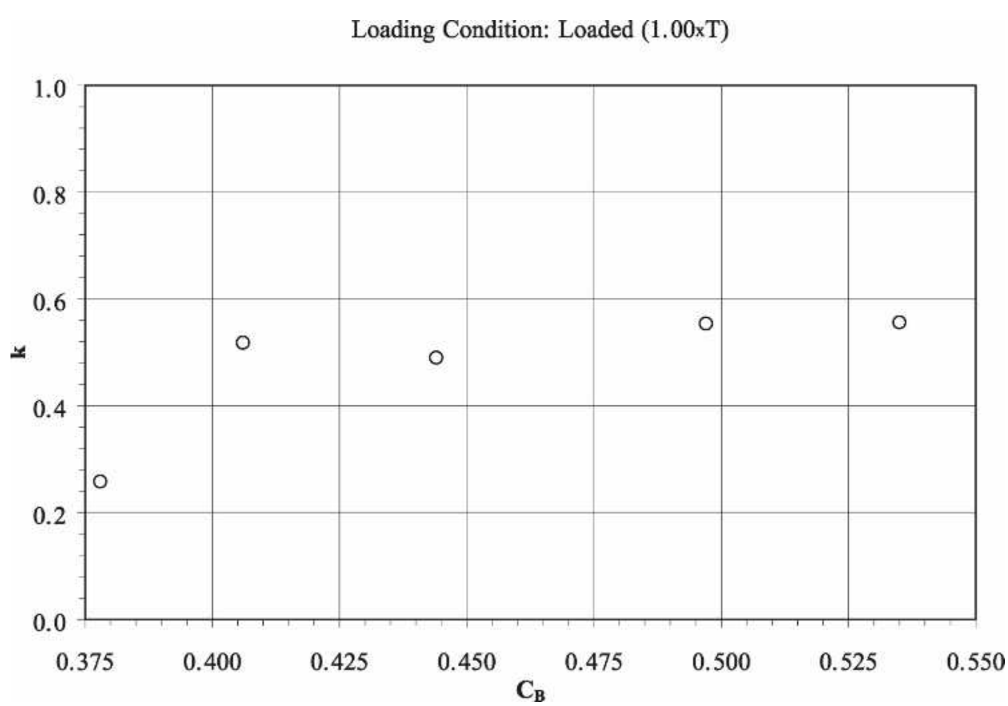

Fig. 10 The distribution of the form factor in the loaded condition

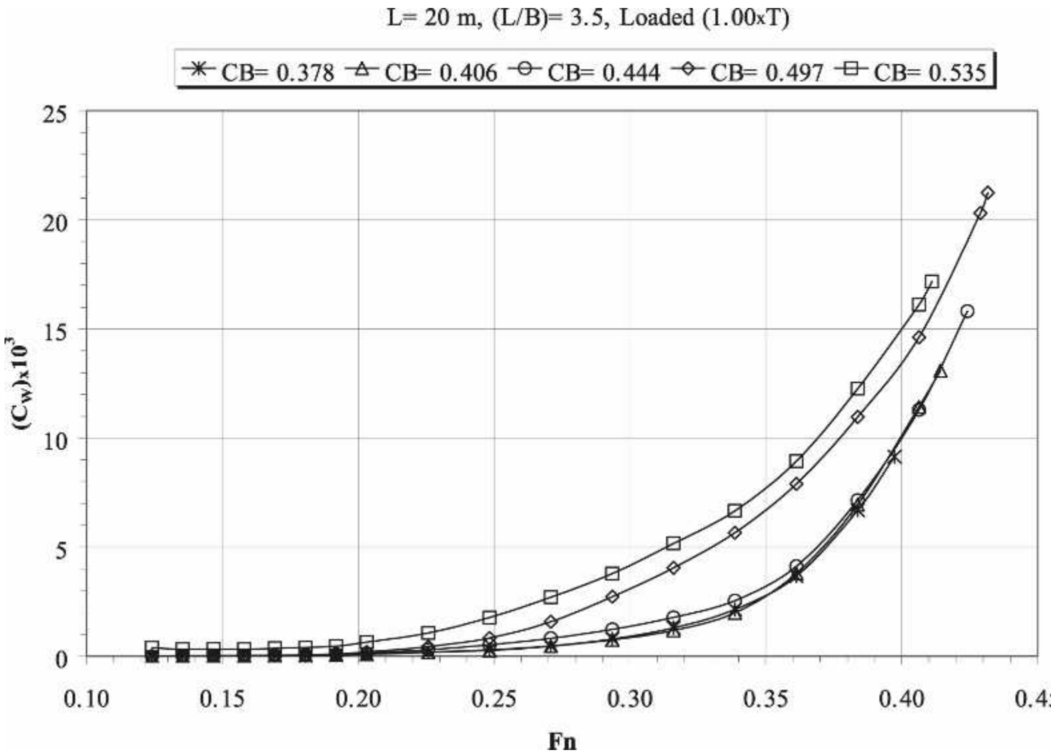

Fig. 11 The wave-making resistance coefficient of the fishing boats with different block coefficients

ship, loaded and highly loaded conditions, the distributions of the form factor with respect to *L/B* are shown in Figs. 12 and 13.

The variation of the wave-making resistance coefficient with the Froude number for the fishing boats 148/3, 148/6, and 148/8 are shown in Fig. 14. Similar results obtained for the fishing boats 148/4, 148/7, and 148/9 are shown in Fig. 15. In both cases, only the results for the loaded condition are presented.

6. Effects of stern type

The effects of stern type on the form factor and the wave-making resistance coefficient were investigated by analyzing

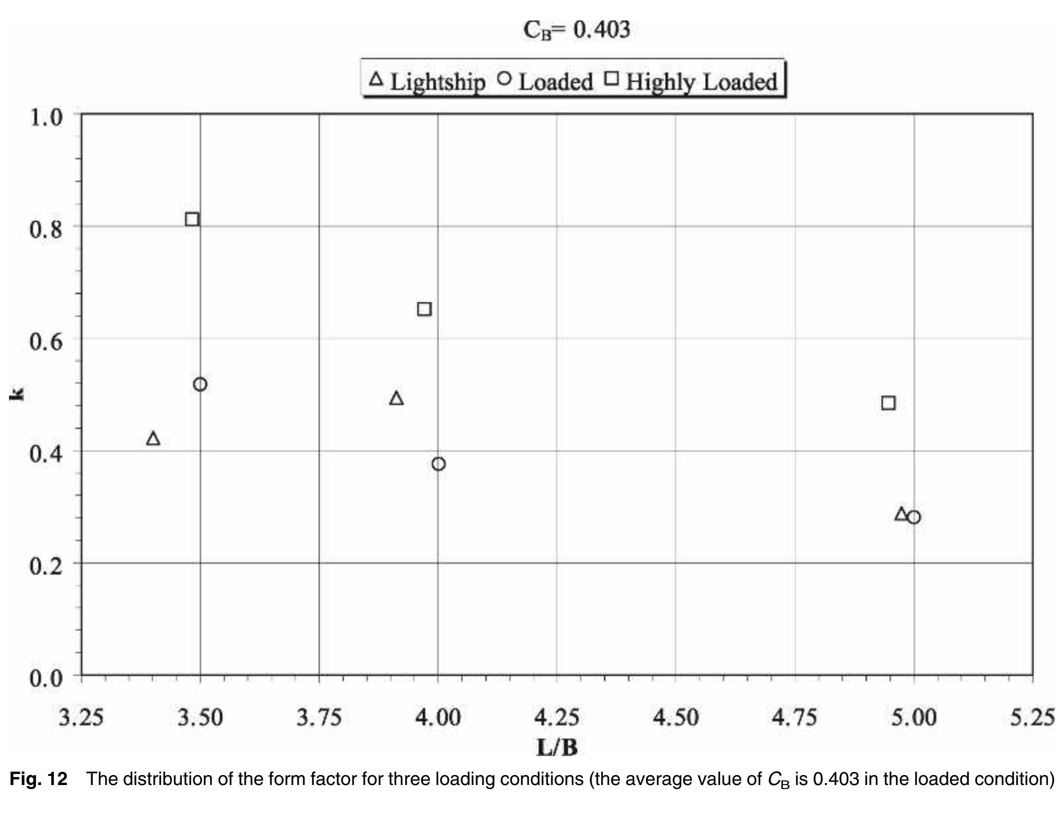

Fig. 12 The distribution of the form factor for three loading conditions (the average value of C_B is 0.403 in the loaded condition)

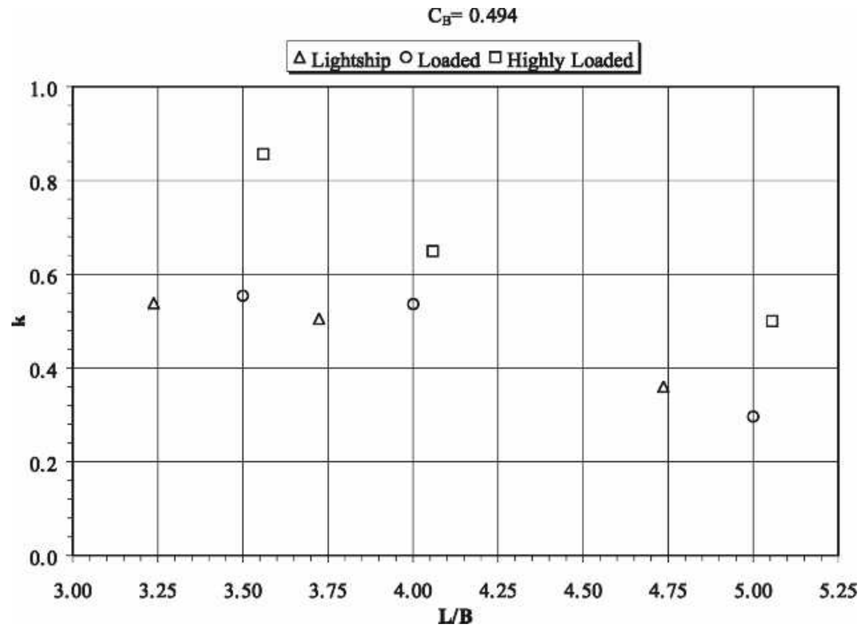

Fig. 13 The distribution of the form factor for three loading conditions (the average value of C_B is 0.494 in the loaded condition)

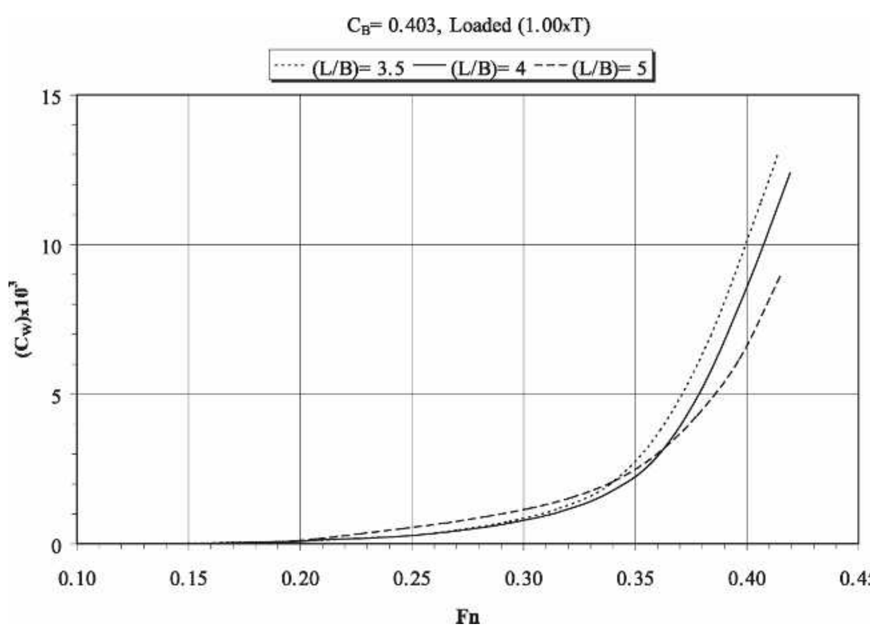

Fig. 14 The variation of wave-making resistance coefficient in the loaded condition (the average value of C_B is 0.403 in the loaded condition)

the resistance tests of the models 148/3B, 148/4B with the transom stern and the models 148/3B(C), 148/4B(C) with the cruiser stern. These models refer to the fishing boats 148/3 and 148/4, respectively, and they are identical with the exception of the stern form. The distributions of the form factor with respect to beam to draught ratio and the stern type are given in Fig. 16 and 17, for C_B = 0.404 and for C_B = 0.498, respectively.

The variations of the wave-making resistance coefficient with the Froude numbers were shown for the fishing boats with both the transom stern and the cruiser stern in the loaded condition. Fig. 18 illustrates the corresponding results for C_B = 0.404, and Fig. 19 illustrates the corresponding results for C_B= 0.498.

7. Effects of chine shape

The effects of the chine shape on the form factor and the wave-making resistance coefficient were investigated using the results of the resistance tests of the model 148/1B. For this purpose, the original chine was modified by rounding as illustrated in Figs. 20 and 21. The tests were carried out in the lightship and loaded conditions. The distribution of the form factor with respect to the beam to draught ratio and the chine shape is given in Fig. 22.

The curves of wave-making resistance coefficient forthe parent fishing boat with the sharp chine and rounded chine in the loaded condition are presented in Fig. 23.

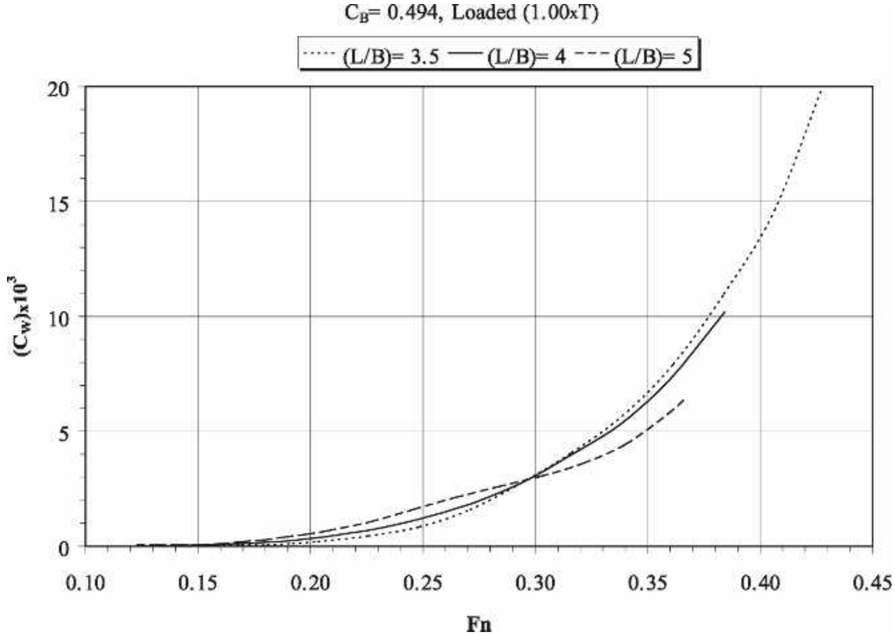

Fig. 15 The curves of wave-making resistance coefficient in the loaded condition (the average value of C_B is 0.494 in the loaded condition)

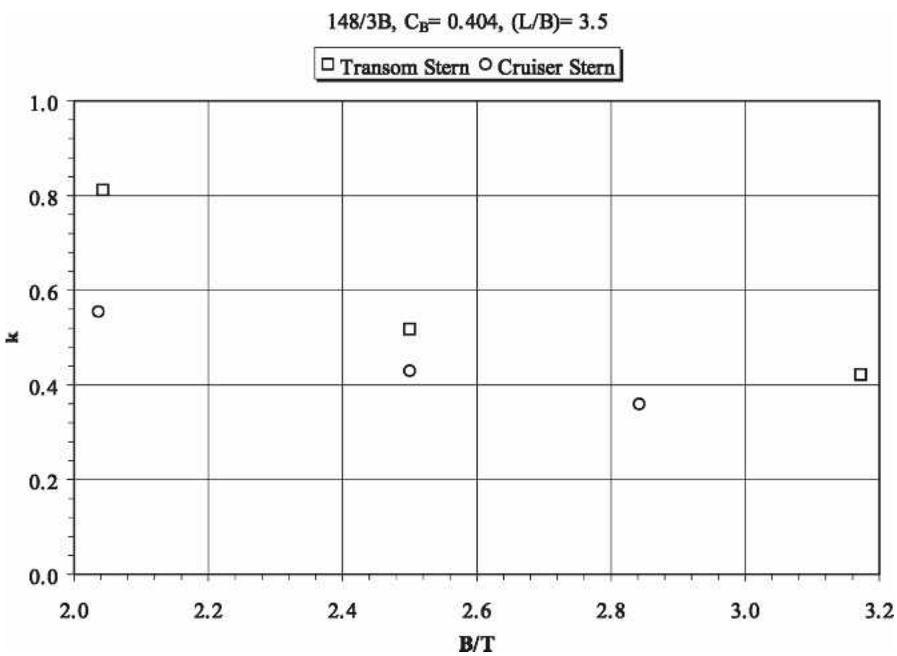

Fig. 16 The variation of the form factor with B/T and the stern type for C_B = 0.404

8. Effects of trim

The effects of trim on the form factor and the wave-making resistance coefficient were examined in the loaded condition by testing models 148/3B and 148/4B in different trim conditions. The details of the trim conditions adopted in the resistance tests are given in Table 5.

The distributions of the form factors obtained for the trimmed and level trim conditions are given in Fig. 24.

The influence of the three trim conditions on thewave-making resistance coefficient is illustrated in Figs. 25 and 26.

9. Effects of appendages

The resistance tests of the geosim models 148/1A, 148/1B, and 148/1C in the lightship, loaded, and highly loaded conditions were repeated with appendages in place. These appendages were the rudder, the heel of the rudder, and the stern tube (see Fig. 6). The distribution of the form factor with respect to the beam to draught ratio for the model 148/1B with appendages and without appendages is shown in Fig. 27.

The curves of total resistance coefficient for the parent fishing boat with the appendages and without appendages at the loaded condition are shown in Fig. 28. The percentages of the C_{Ts} increment due to the presence of the appendages are also given in Table 6 for the loaded condition.

10. Conclusions

By means of the body plans given in this study, a fishing boat of a selected length and block coefficient, which will be

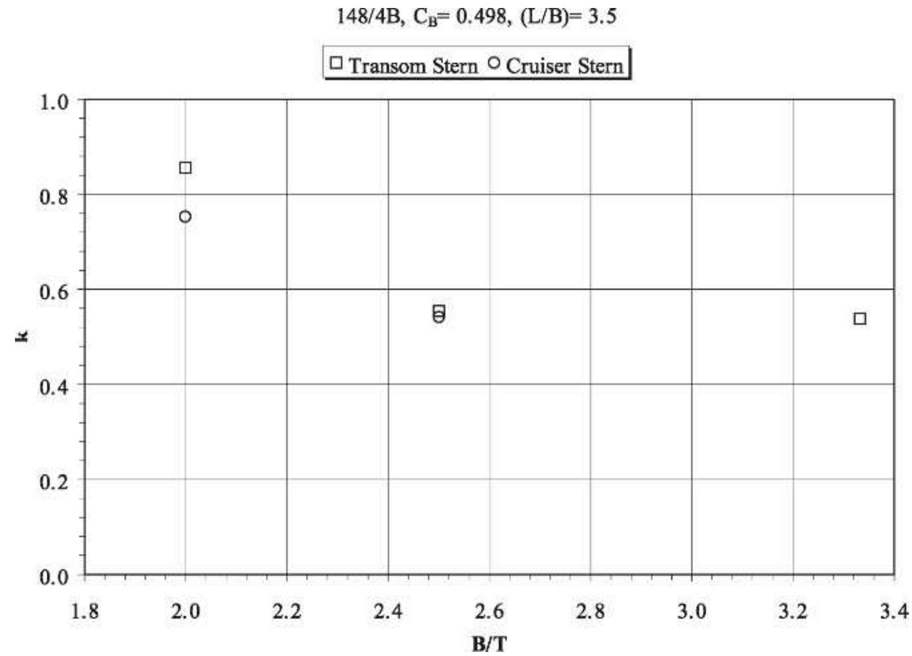

Fig. 17 The variation of the form factor with B/T and the stern type for $C_B = 0.498$

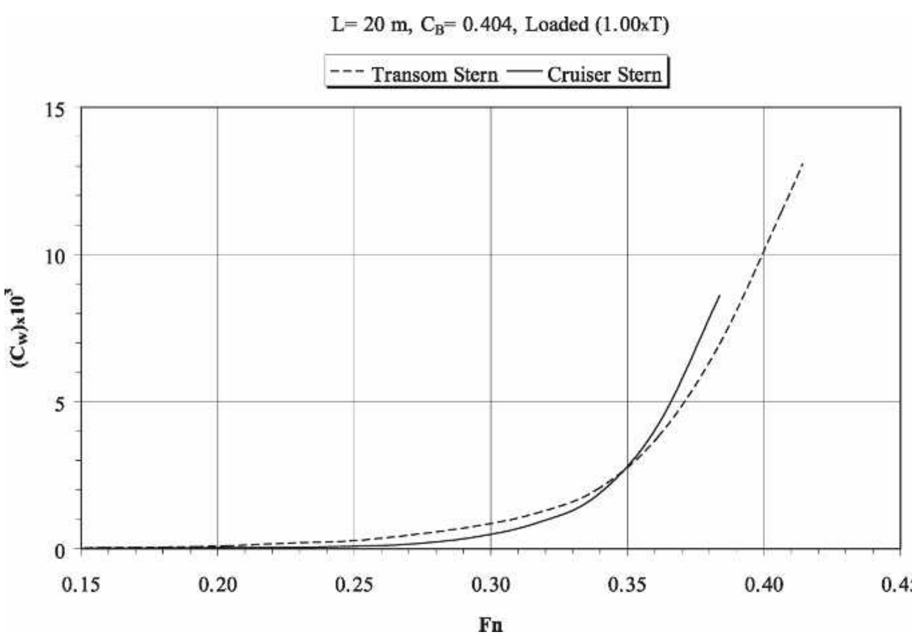

Fig. 18 The curves of the wave-making resistance coefficient for $C_B = 0.404$

capable of operating in the Black Sea, Marmara Sea, Aegean Sea, and the Mediterranean Sea can be obtained.

The present hull form series provides the designer with the value of KG_{max} which satisfies the stability criteria in the lightship and loaded conditions for any derived fishing boat hull.

The conclusions about the resistance characteristics of the Fishing Boat Series are:

- The results of the resistance tests analyses concerning the geosim models with and without appendages indicate that the distribution of the form factor with respect to the RGS value is not regular in all the loading conditions. However, the linear trends of the distribution indicate a decrease. Meanwhile, the form factors obtained with the appendages are larger than the form factors obtained without appendages in all the loading conditions. The scale effects are found to increase by displacement, being the least in the lightship condition and reaching highest values in the heavily loaded condition. The scale effects also increase with the Froude number. The average form factors of the parent fishing boat in the lightship, loaded, and highly loaded conditions are 0.278, 0.289, and 0.525, respectively.
- Concerning the models with the same length but different block coefficient, an increase in the form factor was observed for values of C_B between 0.378 and 0.406. However, for the values of C_B between 0.406 and 0.535, an important variation on the form factor was not seen. This characteristic was also seen both in the lightship and highly loaded conditions, and therefore it may be

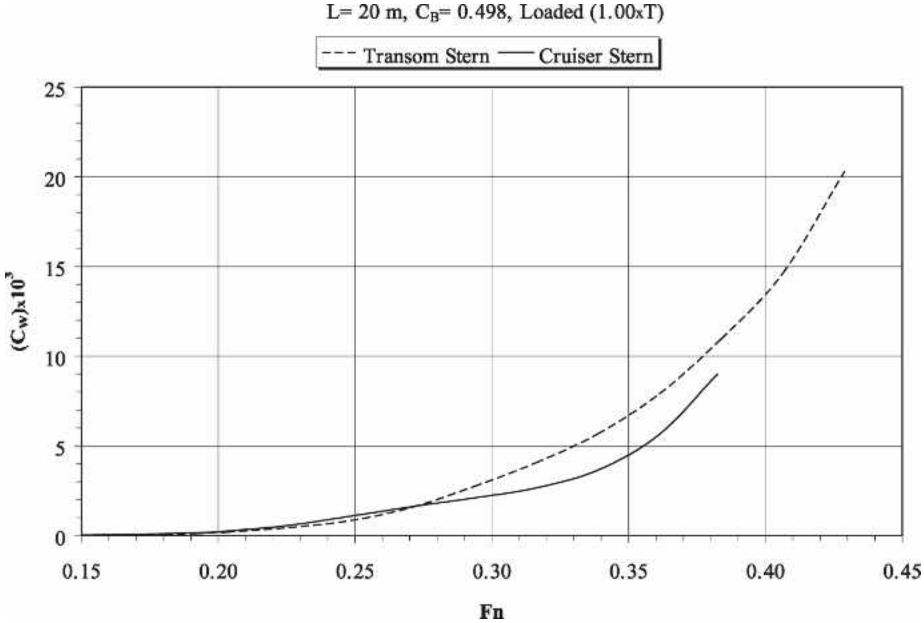

Fig. 19 The curves of the wave-making resistance coefficient for C_B = 0.498

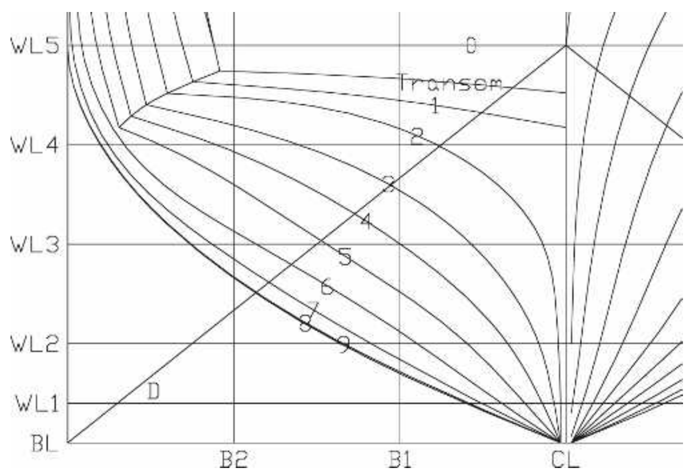

Fig. 20 The sharp chine shape

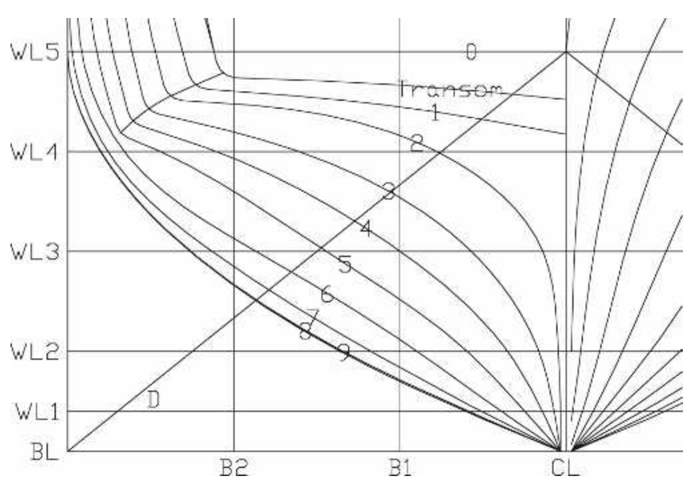

Fig. 21 The rounded chine shape (*R* = 120 mm)

identified as a characteristic of these hull forms. The value of the wave-making resistance coefficient increases if C_B increases in a given loading condition. It is found that within the C_B range from 0.378 to 0.444, acceptable wave-making resistance characteristics are obtained. In fact, this finding can be generalized to the total resistance characteristics of the present series of Fishing Boat Hull Forms.

- In the resistance tests analyses concerning the models with the same block coefficient but different hull length, the value of the form factor decreases if the *L/B* ratio is increased. Furthermore, the C_W values also decrease in all loading conditions if the *L/B* ratio increases, especially for the medium and high values of *Fn*.
- Concerning the models with the transom stern and the cruiser stern, the form factors of the fishing boats with the transom stern are larger with respect to the fishing boats. The wave-making resistance of the fishing boats with the cruiser stern compared with the fishing boats with the transom stern decreases up to the Froude number of 0.347. The average value of the block coefficient for these boats is 0.404. For boats with the average block coefficient 0.498, the same trend is observed, except the limiting *Fn* value is 0.272.
- The fundamental influence of the rounded chine is found to be a degree of increase in the form factor compared to the form with the original chine.
- The investigation into the effects of trim showed that as the block coefficient increased from 0.406 to 0.497, the form factor followed suit specifically in the trimmed by stern condition. However, in the trimmed by bow condition, a decrease in the value of the form factor is observed. In addition, the wave-making resistance values in level trim condition are less than the values in the trimmed conditions for both values of C_B.
- The percentage of the C_W increment due to the appendages decreases for all the loading conditions if the value of *Fn* increases.

The results obtained from the model 148/1C in the wake measurement tests show that:

- The values of the wake coefficient in a large portion of the propeller disk plane are less than 0.1 for all ship speeds employed in the tests.

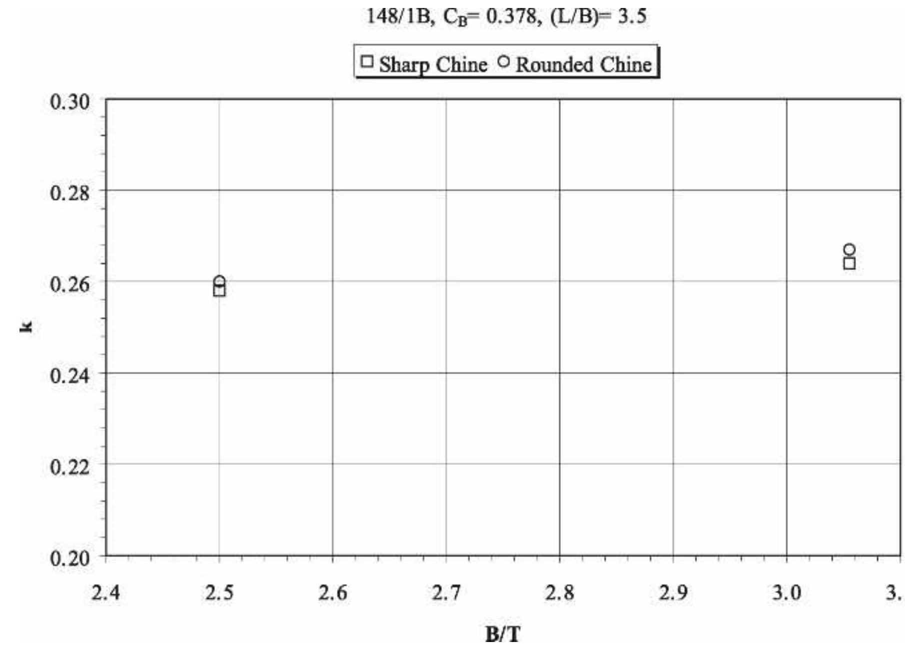

Fig. 22 The distribution of the form factor with respect to the ratio of *B*/*T* and the chine shape

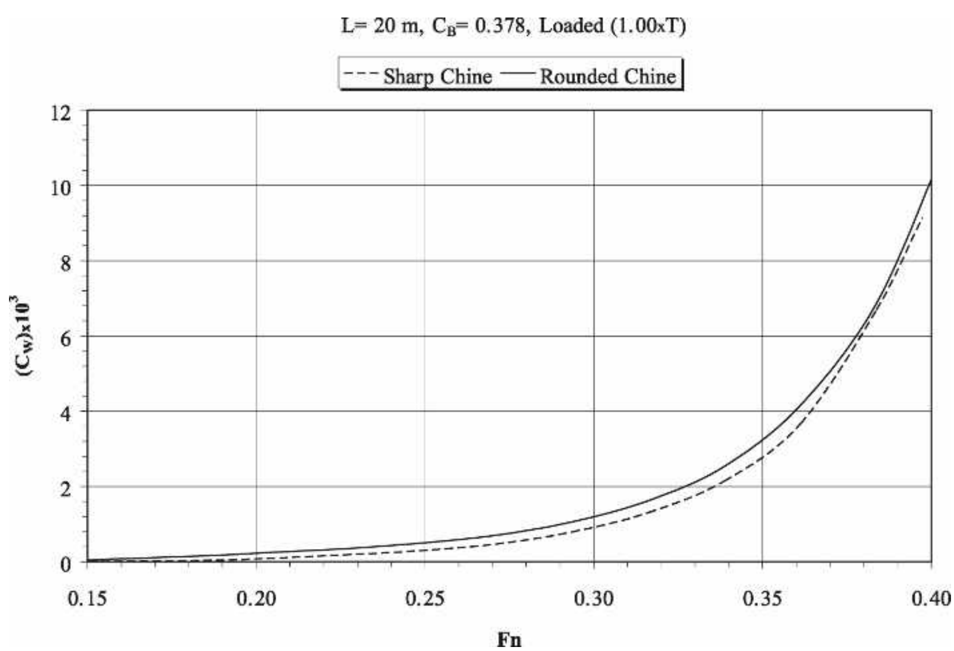

Fig. 23 The curves of the wave-making resistance coefficient for the two different chine shapes

Table 5 The stern and bow draughts and the angles of trim

Model No.	Situation of Trim	Draught at Stern (m)	Draught at Bow (m)	Angle of Trim (°)
148/3B	Trimmed by stern	0.256	0.197	1.7
	Trimmed by bow	0.210	0.256	1.3
148/4B	Trimmed by stern	0.286	0.161	3.6
	Trimmed by bow	1.940	0.261	1.9

- The values of the wake coefficient increase suddenly; in other words, the water velocities decrease suddenly at the upper region of the propeller disk plane up to the hull for all ship speeds employed in the tests.
- The region in which the sudden wake coefficient increase is observed narrows into a smaller triangular area as the ship speed increases.
- The nominal value of the wake coefficient decreases as the ship speed increases.

The results obtained for the model 148/1C in the flow visualization tests are:

1. In the loaded condition (the values of the flow and propeller potentiometers are 110 and 55, respectively):
   - No irregularities are observed in the flow lines in the stations 9, 8.5, and 8.
   - The flow is found to show no irregularities in the region from station 8 to amidships.
   - In the station 2, the flow is normal.
   - In the station 1, there is turbulence in the region over

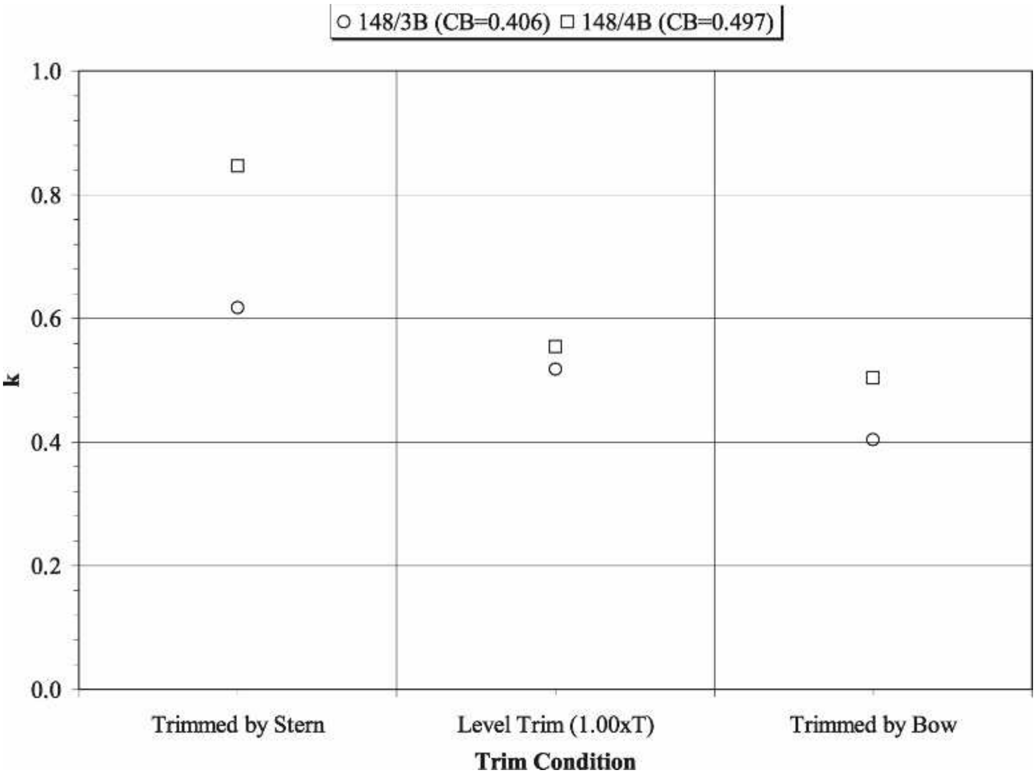

Fig. 24 The distribution of the form factor with respect to the trim condition and block coefficient

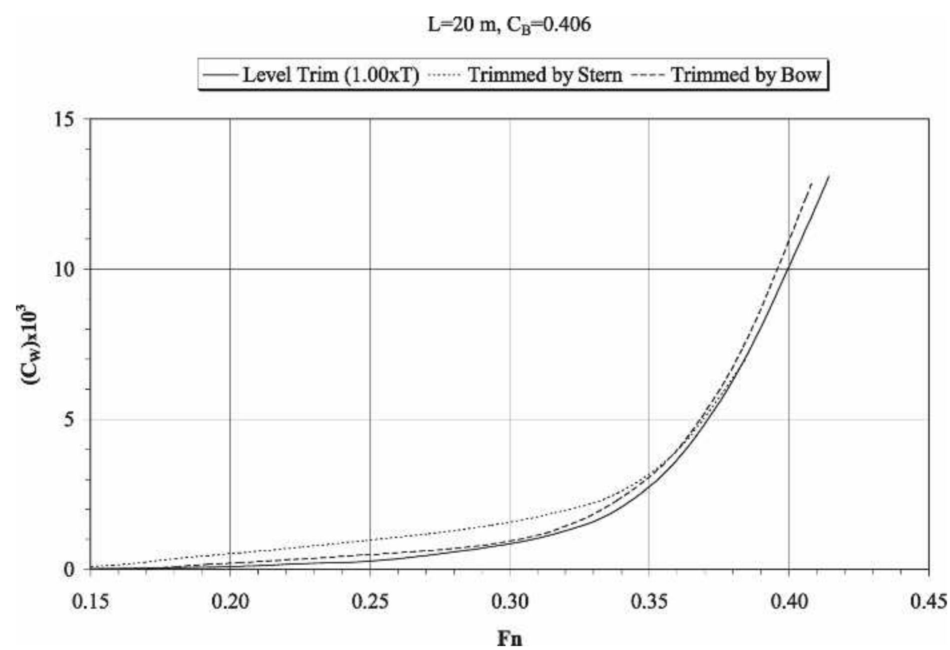

Fig. 25 The curves of wave-making resistance coefficient for the fishing boat 148/3 in the trimmed and level trim conditions

the propeller. Additionally, a suction region over the propeller and a vortex tube are observed at about station 1.

- There is suction in the stations between 1.5 and 1. Here, the tufts oscillate. Some bubbles on the model surface were also observed.
- There is a backward flow on the surface of the hull in the propeller disk plane.
- In the region between the station 0.5 and 0, the flow was dragged tangentially on the hull surface.
- The flow on the rudder is normal.
- The flow in the back of the transom stern is also normal.

2. In the highly loaded condition (the values of the flow and propeller potentiometers are 110 and 55, respectively):
   - A vortex tube occurred over the propeller.
   - In station 0.5, some turbulence was observed in the region over the propeller.

In order to eliminate most of the aforementioned adverse phenomena, it is suggested that a light filling should be ap-

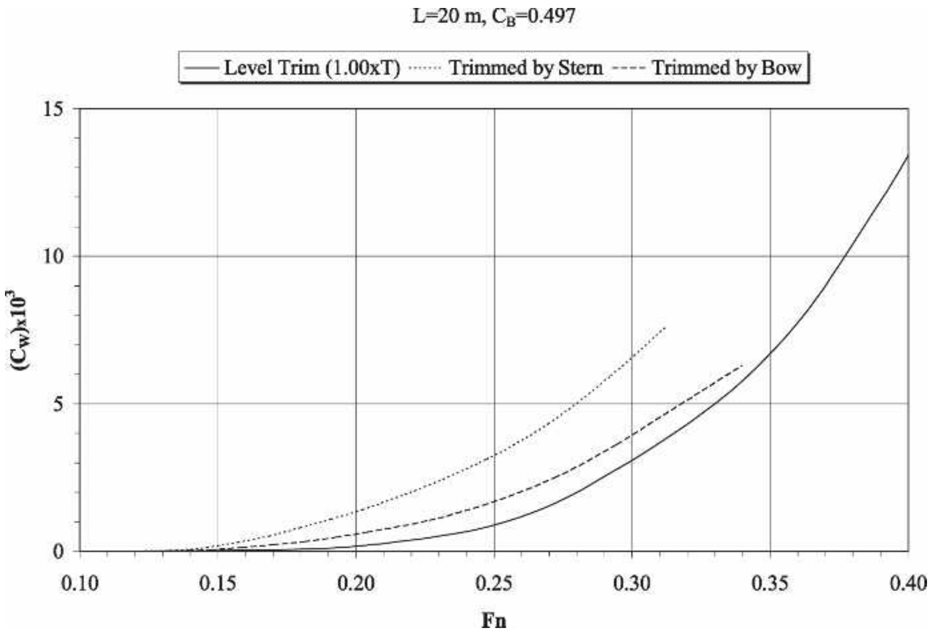

Fig. 26 The curves of wave-making resistance coefficient for the fishing boat 148/4 in the trimmed and level trim conditions

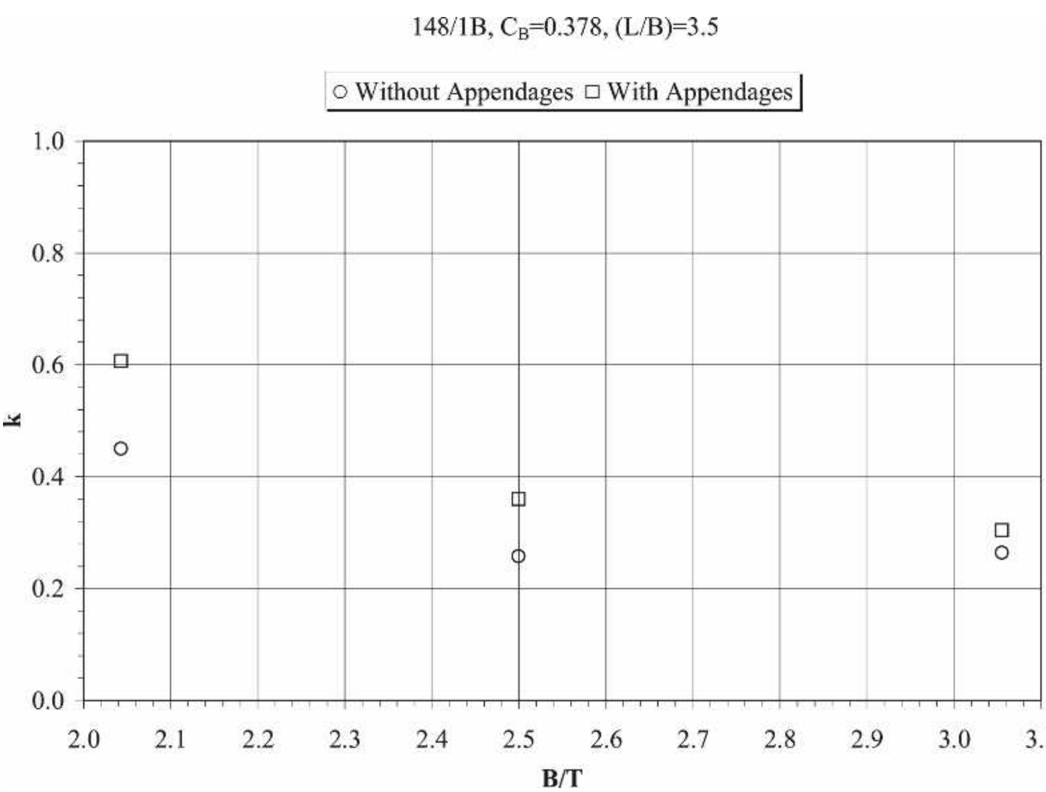

Fig. 27 The distribution of the form factor with respect to the ratio of *B*/*T* and the appendages

plied to the surface between the station 1.5 and 1, thus changing the hull form in that specific area.

The suitable propellers were calculated for the parent fishing boat using the propeller design B_p-δ charts of the Wageningen B 3.50, B 3.65, B 4.40, B 4.55, B 5.45, and B 5.60 series. Subsequently, these propellers were further investigated with a view to satisfy the design criteria such as fitting into the propeller housing, providing the design speed and performing without cavitation, and an optimum propeller was determined for the parent fishing boat. Afterward, using both the B_p-δ and B_u-δ propeller design charts, the RPM value, which provided the maximum open-water efficiency was obtained for the optimum propeller. Finally, the Wageningen B 3.50 propeller at 611 rpm was selected as the optimum propeller.

Acknowledgments

The authors wish to thank Emeritus Professor Kemal Kafali and Associate Professor Omer Belik of Istanbul Technical University.

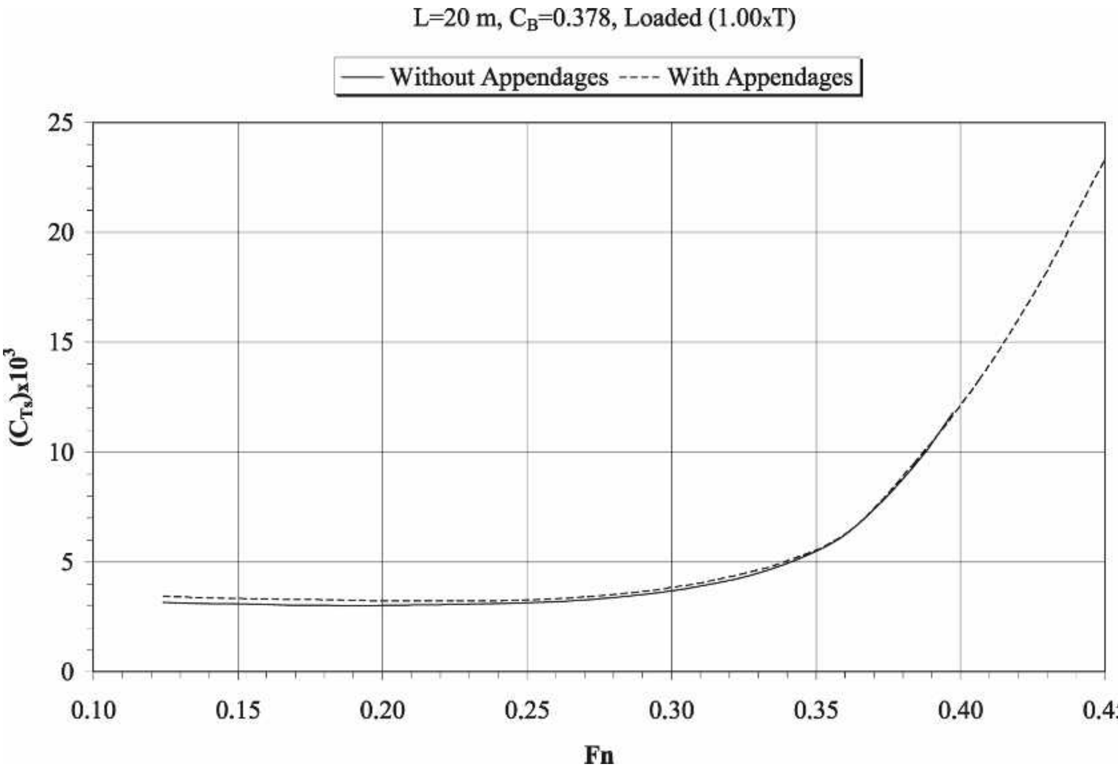

Fig. 28 The curves of the total resistance coefficient for the parent fishing boat in the loaded condition with and without appendages

Table 6 The percentages of the C_{Ts} increment in the loaded condition due to the appendages

Loaded (1.00 × T)	C_{Ts}		C_{Ts} Increment
Fn	Without Append.	With Append.	(%)
0.1242	3.1597	3.4226	8.3
0.1355	3.1197	3.3830	8.4
0.1467	3.0836	3.3432	8.4
0.1580	3.0562	3.3172	8.5
0.1693	3.0298	3.2848	8.4
0.1806	3.0096	3.2634	8.4
0.1919	3.0052	3.2416	7.9
0.2032	3.0138	3.2277	7.1
0.2258	3.0605	3.2251	5.4
0.2483	3.1318	3.2558	4.0
0.2709	3.2686	3.4094	4.3
0.2935	3.5594	3.7023	4.0
0.3161	4.0399	4.1958	3.9
0.3386	4.8508	4.9662	2.4
0.3612	6.3476	6.3562	0.1
0.3838	9.3565	9.4617	1.1

References

Antoniou, A. 1969 *On the Design Characteristics of Greek Type Vessels,* Ph.D. thesis, National Technical University of Athens.

Aydin, M. 2002 *Computer-Aided Design of Fishing Boats Suitable for Turkish Waters* (in Turkish). Ph.D. thesis, Institute of Science and Technology of ITU, Istanbul, Turkey.

Aydin, M., and Akyildiz, H. 2005 Assessment of intact stability characteristics of fishing boats suitable for Turkish waters (in Turkish), *itudergisi/d Engineering,* **4,** 6, Istanbul, Turkey.

Aydin, M., and Salci, A. 2007 Geometrical characteristics of fishing boats series of ITU. Marine Technology, **44,** 2, 125–135.

Doust, D. J. 1959 Resistance and propulsion of trawlers, *Transactions of North-East Cost Engineers, New Castle Upon Tyne,* **75,** 355–436.

Doust, D. J. 1979 Statistical analysis of resistance data for trawlers, *Fishing Boats of the World, London,* **3,** 370–387.

Doust, D. J., Hayes, J. C., and Tsuchiya, T. 1967 A statistical analysis of FAO resistance data for fishing craft, *Fishing Boats of the World,* Volume 3, London.

Hayes, J. C., and Engvall, L. O. 1969 *Computer-Aided Studies of Fishing Boat Hull Resistance,* Fisheries Technical Paper, The Food and Agriculture Organization of the United Nations.

Kafali, K. 1980. *Study of Hull Forms of Fishing Boats* (in Turkish), Ship Institute of ITU, Number 25, Istanbul, Turkey.

Kafali, K., Saylan, O., and Salci, A. 1979 *Development of Hull Forms of Fishing Boats Suitable for Turkish Waters* (in Turkish). The Scientific & Technological Research Council of Turkey, Project Number G-416, Istanbul, Turkey.

Kalipci, S. 1995 *Systematic Resistance Analyses of Infantry Type of Fishing Boats* (in Turkish), B.Sc. thesis, Naval Architecture and Ocean Engineering Faculty of ITU, Istanbul, Turkey.

Kalipci, S. 1999 *Hydrodynamic Analyses of Infantry Type of Fishing Boats* (in Turkish). M.Sc. thesis, Institute of Science and Technology of ITU, Istanbul, Turkey.

Kukner, A., and Aydin, M. 1997 Influence of design parameters on vertical motions of trawler hull forms in head seas. Marine Technology, **34,** 3.

Kucuk, F. 1964 *Resistance Characteristics of Cektirme* (in Turkish), Ph.D. thesis, Faculty of Mechanical Engineering of ITU, Istanbul, Turkey.

Nutku, A. 1957 Model tests with fishing boats (I). *Bulletin of ITU Ship Institute,* **3,** Istanbul, Turkey.

Nutku, A. 1962 Model tests with fishing boats (II). *Bulletin of ITU Ship Institute,* **7,** Istanbul, Turkey.

Prifti, A. C., and Grigoropoulos, G. J. 1995 Resistance characteristics of the traditional Greek fishing vessels, *Proceedings,* Fifth International Symposium on Techniques and Technology in Fishing Vessels, Athens.

Ridgely-Nevitt, C. 1956 The resistance of trawler hull forms of 0.65 prismatic coefficient, *Transactions of the Society of Naval Architects and Marine Engineers,* **64,** 433–468.

Ridgely-Nevitt, C. 1963 The development of parent hulls for a high displacement-length series of trawler forms, *Transactions of the Society of Naval Architects and Marine Engineers,* **71,** 5–30.

Salci, A. 1985 Power calculations of fishing boats (in Turkish), *Proceedings,* Seminars of Spring Semester 1984–1985, Institute of Marine and Technology of Dokuz Eylul University, Izmir, Turkey.

Van Oortmerssen, G. 1973 A power prediction method for motor boats, *Proceedings,* Symposium Yacht Architecture, HISWA'73.

Van Oortmerssen, G. 1980 A power prediction method and its application to small ships, *Proceedings,* Naval Architecture Course Notes, Delft University, Delft.